International Journal of Green Energy

ISSN: 1543-5075 (Print) 1543-5083 (Online) Journal homepage: www.tandfonline.com/journals/ljge20

The Optimized Operation of a Solar Hybrid Desiccant/Displacement Ventilation Combined with a Personalized Evaporative Cooler

Mohammad Hammoud, Kamel Ghali & Nesreen Ghaddar

To cite this article: Mohammad Hammoud, Kamel Ghali & Nesreen Ghaddar (2014) The Optimized Operation of a Solar Hybrid Desiccant/Displacement Ventilation Combined with a Personalized Evaporative Cooler, International Journal of Green Energy, 11:2, 141-160, DOI: 10.1080/15435075.2013.771360

To link to this article: https://doi.org/10.1080/15435075.2013.771360

Published online: 28 Aug 2013.

International Journal of Green Energy, 11: 141–160, 2014

ISSN: 1543-5075 print / 1543-5083 online
DOI: 10.1080/15435075.2013.771360

Taylor & Francis
Taylor & Francis Group

THE OPTIMIZED OPERATION OF A SOLAR HYBRID DESICCANT/DISPLACEMENT VENTILATION COMBINED WITH A PERSONALIZED EVAPORATIVE COOLER

Mohammad Hammoud, Kamel Ghali, and Nesreen Ghaddar
Department of Mechanical Engineering, American University of Beirut, Beirut, Lebanon

The study investigates by modeling and experimentation the performance of displacement ventilation (DV) aided with personalized evaporative cooler (PEC) system that operates in humid climate and uses a solid desiccant (SD) dehumidification system regenerated by parabolic solar concentrator thermal source. Predictive component models of the conditioned space, the SD, the solar concentrator system, and the PEC were developed and used for the prediction of associated operational energy consumption while utilizing an optimized control strategy. The control strategy seeks optimal values of supply air flow rate and temperature and the desiccant regeneration temperature for both cases with and without the aid of the PEC while meeting space load, indoor air quality, and thermal comfort requirements. Energy consumption was calculated for the optimized strategy using genetic algorithm optimizer and the integrated DV/SD-PEC models. The results agreed well with experimental data obtained from tests on a DV climatic chamber. In addition, votes of comfort recorded by participants in the experiment using PEC were very similar to predicted comfort. The optimized hybrid system performance was applied to a typical office space of area of 64 m^2. The operation of the hybrid system with PECs resulted in a higher supply air temperature. The increment in supply air temperature is 1.1°C when PEC is used compared to case without PEC. This increase in temperature showed that an energy saving of 13.5% is achieved for the PEC aided hybrid system.

Keywords: ***Desiccant dehumidification; Hybrid air conditioning systems performance; Optimized air conditioning control strategy; Displacement ventilation; Personalized evaporative cooler***

INTRODUCTION

The displacement ventilation (DV) system has become popular over recent years for its improved indoor air quality (IAQ) and low energy consumption (Jiang, Chen, and Moser 1992; Yuan, Chen, and Glicksman 2001). The DV system provides the supply fresh air at low level and relies on buoyancy to drive the contaminants upward. Consequently, it divides the space into two regions: lower occupied fresh and cool air zone and an upper contaminant zone above the breathing level of occupants (Mossolly et al. 2008). To ensure thermal comfort, the supply air temperature of a DV air conditioning system is usually greater than 18°C and the acceptable supply velocity is less than 0.2 m/s to prevent any

Address correspondence to Kamel Ghali, Department of Mechanical Engineering, American University of Beirut, P.O. Box 11-0236, Beirut 1107- 2020, Lebanon. E-mail: ka04@aub.edu.lb

possible thermal draft in the occupied zone. These two constraints, relatively high supply air temperature and low air velocity, not only limit the application of the DV system to low cooling loads of less than 40 W/m^2 but also decreases the system's energy efficiency in hot and humid environments. Moreover, in humid climates the DV system may not be cost effective since outdoor humidity is a major contributor to energy inefficiency if 100% fresh air is used. The high humidity of the outside air combined with ventilation requirement increases the latent load and would jeopardize the effectiveness of the DV system that requires relatively dry supply air. In fact satisfying these constraints requires a large amount of energy to cool and dehumidify the air and a substantial amount of reheat energy to bring the temperature of the DV supplied air to at least 18°C. Such limitations have encouraged researchers to consider various alternatives to increase the load capacity of the DV system to cooling loads, which exceeds the limit of 40 W/m^2 and to minimize the system ineffectiveness in hot and humid climates.

Researchers have considered DV with the use of desiccant dehumidification, which relies on the concept of removing the humidity by absorption rather than sub-cooling and the use of heat energy to regenerate the desiccant system. The use of desiccant pre-conditioning of supply air is a viable alternative to independently control the humidity and air temperature to improve overall energy efficiency of the system and reduce energy costs (Meckler 1995; Ghali, Othmani, and Ghaddar 2008; Xiong, Dai, and Wang 2010). The dehumidification cost is high if conventional cooling coil with reheat is used. The incorporation of solid desiccant (SD) pre-conditioning into such systems allows a higher percentage of fresh air in the supply stream at lower energy cost (Fang, Clausen, and Fanger 1998; Ayoub, Ghaddar, and Ghali 2007). Since the desiccant system is a heat-driven cycle, then it has the potential to use low density energy, such as natural gas, waste heat, and solar energy (Ahmed, Kattab, and Fouad 2005; Chung, Lee, and Yoon 2008). The use of desiccant system improves the efficiency of the DV system. It is reported that the desiccant cooling system has an operational cost that is less than one-third of energy consumed in conventional air conditioning system (Audah, Ghaddar, and Ghali 2011), due to the increase in sensible cooling caused by the use of heat in the dehumidification process.

In view of the fact that desiccant system allows the delivery of the supply air at higher temperature and to introduce more energy savings to the hybrid DV/SD system, other researchers used personalized cooling to prevent lowering the supply air temperature and enhancing the system's efficiency and load coverage (Makhoul, Ghali, and Ghaddar 2013). Personalized evaporative cooling (PEC) is based on the concept of localizing the fresh air rather than mixing it with space return air as the case with conventional air conditioning systems. It aims to supply clean air direct to the breathing zone of occupants and to provide the occupant with the opportunity of controlling his own microenvironment (Melikov 2004). Furthermore, it provides cooling for the upper part of the human body, which has a significant effect on the overall comfort. It was shown that integrating a ductless PEC system in a DV cooled space while using the lower clean and cool air of the DV system and supplying it to the breathing zone of the occupant may improve thermal comfort and result in energy savings. An estimated energy savings up to 20% was reported from using higher supply air temperature in the DV system aided with PEC while maintaining thermal comfort (Makhoul, Ghali, and Ghaddar 2013).

It is evident that enhancing the overall efficiency of a DV system in hot and humid climates requires integration with a desiccant system dehumidification that is powered by solar energy and the use of personalized evaporative cooling to reduce the energy required for cooling the supply air. Since more than three subsystems are used with independent

energy sources for the removal of sensible and latent loads and for providing localized comfort, there is a major need to optimize the operation of these different subsystems for effective performance of the DV in hot and humid climates. The objective of this work is to optimize the operation of the integrated DV cooling system, SD dehumidification, and the PEC subsystems to provide comfort and good environmental quality in the breathing zone at minimal energy cost for an office space in the city of Beirut. The optimization problem for the control of the hybrid cooling system operation will be formulated based on minimizing energy consumption cost of system components using genetic algorithm search method to solve for the optimal operational set points under transient load for the DV supply flow rate and temperature and SD regeneration temperature.

SYSTEM DESCRIPTION

The hybrid air conditioning system is composed of a desiccant wheel, a sensible wheel, a cooling coil, a regenerative coil, a variable speed fan, parabolic solar collectors, an auxiliary heater, and PECs. Figure 1 illustrates the system components.

The processed air is supplied by an air handling unit (AHU) that integrates the desiccant and sensible wheels, the cooling and regenerating coils, in addition to the synchronized supply and return fans. The AHU draws outside air at state (1) and passes it through a desiccant dehumidification wheel where it loses part of its moisture content and heats up. Exiting the desiccant wheel at state (2), the air stream releases some of its heat energy to the return air through the use of a sensible wheel and finally the processed air is admitted to the space at state (4) after decreasing its temperature to the desired supply temperature. Inside the space, the cool supply air picks the load and contaminants from

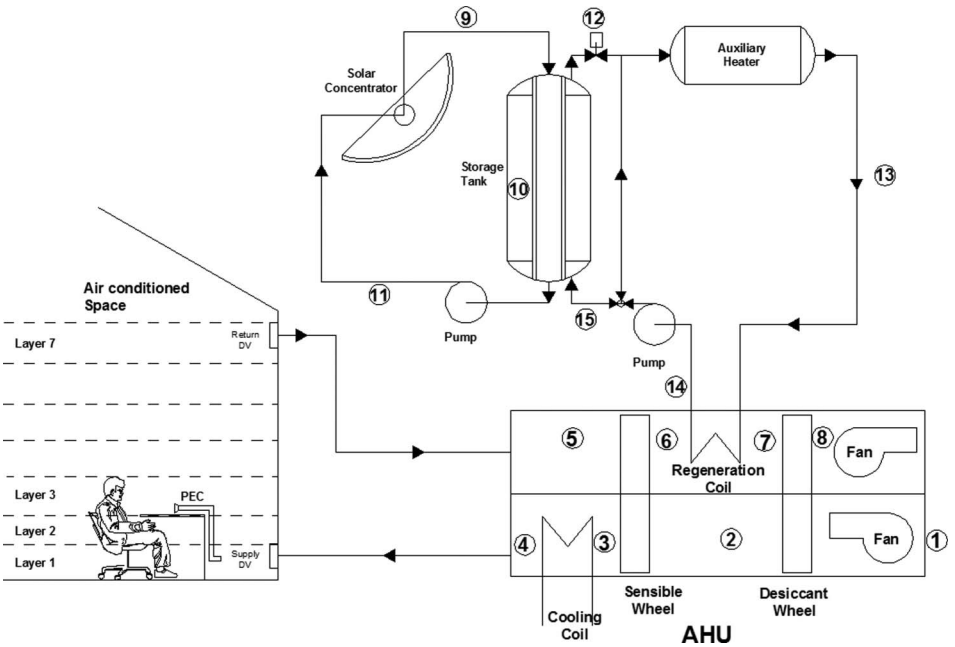

Figure 1 Schematic of the hybrid air conditioning system.

the space before it leaves the space at state (5) to be heated by the sensible wheel and the regeneration coil to regenerate the desiccant wheel before it exits the AHU at state (8).

The heat input needs of the regeneration coil are provided partly by parabolic solar concentrators and by an auxiliary heater. The solar concentrators system is used because it occupies smaller roof area compared to flat plate collector system and is able to sustain longer hours of high-grade energy (Ahmed, Kattab, and Fouad 2005). Depending on the temperature of water leaving the regeneration coil at state (14) and the temperature of the water inside the storage tank at state (10), the three-way valve will either direct the water leaving the regeneration coil to the solar heated storage tank or to the auxiliary heater.

Finally, a PEC is used in conjunction with the DV air conditioning system. The PEC draws the fresh air supplied over the floor to lower its temperature by humidification and then directing it to the upper body part of the occupant, the most comfort sensitive body part. The PEC will be constantly supplying cool air, it is mainly used to assist the DV system in providing thermal comfort at lower energy cost and to simultaneously provide the occupant with the mean of controlling his own thermal comfort needs.

MODELING METHODOLOGY

A first step to formulate the optimization problem based on operating cost is to integrate simulation models for the space thermal response to the DV cooling, the fan coil unit (air handling unit), the SD wheel, the regeneration coil, the PEC, the solar concentrator and the storage tank thermal response, and suitable performance prediction models of water chiller, fans, and pumps. The simulation model of space, system, and components should be capable of predicting space vertical temperature gradient including micro climate environment around the head and trunk when PEC is used, space stratification height and associated DV system performance parameters subject to time-varying loads in the space. In addition, a segmental bioheat model is needed to predict segmental skin temperatures and their rate of change to be used for the assessment of local and overall comfort of the occupant.

The optimizer development aims at finding the optimum setting of the design operational variables on an hourly basis and at simultaneously achieving thermal comfort and IAQ at minimum power consumption for the total 12 hours of system operation from 7 a.m. till 7 p.m. The optimization of DV system operation for a single or a number of spaces operated by a specific control strategy is a complex task that requires the minimization of the operational energy cost over the cooling season months. To be able to calculate the operational cost of the DV system, the following steps are followed:

1. The cooling load requirement of the space(s) shall be defined along with the detailed physical and geometrical parameters of the space(s) including the intended choice of the system control strategy.
2. The base control strategy (strategy A) is represented by a variable DV supply air temperature, DV supply air flow rate, and regeneration air temperature at fixed PEC air flow rate. This strategy is used when system sizing and operation is done with the expected utilization of the PEC. A sub-control strategy is also considered for the removal of the space load without the use of the PEC (strategy B).
3. The equipment capacity of the DV sub-systems (chiller, dehumidification wheel, and solar concentrators) was sized based on peak load conditions for both cases when PEC is used or the PEC is not used.

4. The DV system must meet both thermal comfort constraint air quality constraints. These constraints associated with the system physical model are: (1) thermal comfort level must be above −0.5 for the nine-point thermal comfort scale that runs from very uncomfortable (−4) to very comfortable (+4) and (2) the minimum permissible stratification height H is 1.0 m. This constraint ensures that the IAQ meets ASHRAE standard (2007) of CO_2 concentration level less than a threshold value of 1000 ppm in the occupied zone. To ensure that these constraints are met, we will use the segmental bioheat model of Salloum, Ghaddar, and Ghali (2007) to predict occupant thermal response and then use the model of Zhang (2003) to evaluate local and overall comfort associated with space environmental conditions sustained by the DV system. The air quality, measured by the stratification height is determined from the DV-conditioned space model of Makhoul, Ghali, and Ghaddar (2012).
5. Define the overall cost function represented by five elements that account for fan energy, cooling coil energy, auxiliary heating energy, thermal comfort cost, and minimum allowed stratification height cost over the optimization prediction or sampling period (Caldas and Norford 2003).
6. Use a derivative-free genetic algorithm optimizer that searches through the different possible control variable settings during a specific operating period to determine the optimized control variable set points, which minimizes the energy cost while maintaining the space requirements: load, comfort, and IAQ for the total hours of the air conditioning system operation. The choice of genetic algorithm arises from its robustness and in being acceptably good in finding near optimum solutions (Mitchell 1997). Genetic algorithm is most efficient when the optimization problem is not uni-modal or when the cost function is noisy.

Since several mathematical models are integrated to simulate the hybrid system operation, it becomes important to validate the integrated model results and ensure that thermal comfort predictions are correct. The validation will be done by performing two types of experiments: the first is concerned with predicted energy performance for given operational set points; and the second by conducting an occupant survey in which participants record their votes on the attained comfort level. In the next section, we will present briefly the mathematical models and the optimization methodology that will be followed by a description of the experiments.

Mathematical Models

To determine the performance of the integrated hybrid system under optimized conditions during transient operation, a set of mathematical models of the various mechanical subsystems are integrated to predict the space and thermal comfort conditions as well as the system energy consumption. The details of the models will not be provided here, but they will be referenced as follows:

Displacement ventilation space model. The quasi-steady DV model developed by Makhoul, Ghali, and Ghaddar (2012) is used in this work. The model assumes unidirectional vertical air movement and therefore divides the space into seven horizontal layers, the first three levels are designed according to the human body segment sizes and the last four levels are divided equally for the remaining distance. In each layer, the model identifies three different air temperatures for the wall plume, heat source plume, and the surrounding air.

To simulate the indoor environmental conditions subject to internal and external loads, Makhoul, Ghali, and Ghaddar (2012) integrated the DV with a space thermal model. The integrated DV-space model requires the outdoor weather conditions (dry bulb temperature, wet bulb temperature, wind velocity, and solar radiation) as input data to determine the wall internal surface temperatures. This information is necessary to compute the plume flow rates of the heat source and walls as well as the space air temperature in the different layers.

Personalized evaporative cooler model. The cool air supplied by the PEC is directed to the human body upper segments and thus affecting the occupant segmental thermal comfort. The outlet air stream temperature of the evaporative cooler depends on the inlet air stream's humidity ratio, temperature, and the flow rate of the evaporative cooler. There are many types of PECs depending on the method of introducing water in air and PECs are commercially available products that are battery operated. The mass and energy balances will vary depending on the mechanism of wetting and evaporation of water vapor in air. In this work, we chose to use a published performance correlation for commercially tested and available water cooling-pad-type PEC. The experimental correlation of Chakroun, Ghaddar, and Ghali (2011) for the water cooling-pad-type PEC is adopted and it is represented by the following equation:

$$T_{\mathrm{PEC}} = -0.024 q_{\mathrm{PEC}} + 1.28 T_{\mathrm{in}} + 0.127 \mathrm{RH}_{\mathrm{in}} - 12.563, \tag{1}$$

where T_{PEC} is the outlet temperature of the PEC jet in (°C), q_{PEC} is the volumetric flow rate in (l/s), T_{in} is the inlet temperature in (°C), and $\mathrm{RH}_{\mathrm{in}}$ is the relative humidity at the inlet of the PEC. However, the PEC outlet diameter is 5 cm and it is located at $x = 70$ cm from the face. This correlation was tested under flow rates ranging between 4 and 14 l/s and inlet temperature conditions of 21–25°C at intervals of 1°C with relative humidity not exceeding 51%.

The bioheat and thermal comfort modeling. This work implements the bioheat model developed by Salloum, Ghaddar, and Ghali (2007) to evaluate the thermal comfort of the occupant. The model divides the body into 11 segments (head, chest, back, abdomen, buttocks, upper arm, lower arm, hands, thighs, calves, and feet) and determines segmental skin temperatures of the body segments, which influence the rising thermal plume. The segmental and overall thermal state of comfort is predicted based on Zhang's model (2003) for transient and non-uniform thermal environments.

Desiccant wheel model. The desiccant wheel is divided into two sections: regeneration and dehumidification section to simultaneously dehumidify the processed air and regenerate the desiccant. The rotary regenerative wheel exposes one section of the desiccant material to the humid fresh air stream, while the regeneration air steam passes the other wheel section simultaneously in a counter flow arrangement. As a result, the processed air exiting the dehumidification section undergoes an increase in temperature but with a decrease in its humidity, and on the other side the regenerative air stream exits the wheel with a lower temperature but higher humidity. We use the one-dimensional model of Zheng and Worek (1993) of coupled heat and mass transfer for a rotary dehumidifier to predict the temperature and humidity profiles of the two air streams. The model has shown to yield good results when used in other research works (Ayoub, Ghaddar, and Ghali 2007) and hence it will be used in the current work. The simulation of the desiccant model requires the following input parameters: conditions of the process air at state (1),

conditions of regeneration air at state (7), rotational speed of the wheel, wheel dimensions, and air velocity. The simulations of the coupled equations will result in the temperature and humidity ratio of the air leaving the desiccant wheel at state (2) and the regenerating air leaving the desiccant wheel at state (8).

Solar concentrator model. To determine the portion of solar heat provided for regenerating the desiccant, the transient performance of the solar concentrator and storage tank is simulated using the model presented by Duffie and Beckman (2003). A well-mixed storage tank model is used in which the concentrator circuit coil is embedded. The calculated useful heat gain Q_u will be then used in determining the water transient temperature inside the storage tank for the required load extracted from the tank by water circuit before entering the regenerator coil.

The above models will be integrated and then will be coupled to a genetic algorithm optimizer that seeds the simulation models with different sets of operational variables to select the values that would set the integrated system to the optimal operating point that minimizes the energy consumption and satisfies the constraints of thermal comfort and air quality.

Optimization Tool

The hybrid system components are integrated with the space dynamic component models to calculate the associated power consumption for the given operational design parameters: regeneration temperature, supply air flow rate, and temperature. The optimizer development aims at finding the optimum setting of the design operational variables while meeting constraints of comfort and IAQ on an hourly basis based on minimizing the cost function J for the total hours of system operation. The objective cost function is given by

$$J = \alpha_H I'_H + \alpha_S I'_S + \alpha_{\mathrm{f}} I_{\mathrm{f}} + \alpha_{\mathrm{c}} I_{\mathrm{c}} + \alpha_{\mathrm{aux}} I_{\mathrm{aux}}, \tag{2}$$

where I_{c} is the cooling coil energy, I_{f} is the fan energy consumption, and I_{aux} is the regeneration coil energy consumption, the stratification and thermal sensation constraints are represented in the form of I_S and I_H, respectively. The weighting factors, α's are applied on each term to represent its priority. These factors may be changed repetitively while running the genetic algorithm so that the best combination of these weighting factors is reached for a convenient performance of the system (Wright, Loosemore, and Farmani 2002). The stratification height cost term I'_H represents the normalized deviation from the set minimum stratification height given by

$$I'_H = \exp\left(\frac{H_{\min}}{H}\right) - 1. \tag{3}$$

The weighting factors, α, are selected such that all the elements have important contribution and are given in Table 1.

When using genetic algorithms for multi-objective optimization, weighing factors are internally assigned to the different variables (Knoak et al. 2006). The assigning of weights is done to reduce the computational time. Moreover, not all constraints will have the same importance in our analysis. There are two types of weighting factors that appear in the objective function (see Eq. (2)): (i) the weighting factors for the cost functions and (ii) the weighting factors for constraint functions. The weighting factors for the cost functions are simply the factors of conversion that convert the energy to the cost in dollars. For the

Table 1 Weighting Factors Values

Weighting factor	Description	Value
α_H (\$)	Stratification height weighing factor	1
α_S (\$)	Thermal sensation weighting factor	100
α_c (\$/W)	Cooling coil weighting factor	1
α_f (\$/W)	Fan weighting factor	1
α_{aux} (\$/W)	Auxiliary heater weighting factor	1

constraints, the weighting factors are chosen such that the constraints are comparable to the cost (in dollars). As an example if the cost in dollar is in the order of 100 and thermal sensation is of an order of unity, then a weighing factor of 100 is chosen to make the numbers comparable so that the optimization is meaningful. The choice of α's for the constraint terms is done after few trials.

The optimization of the integrated model is solved using genetic algorithm procedures implemented on MATLAB (Zheng and Zaheer-Uddin 1996) to identify the pay-off characteristics between daily energy cost, zone thermal comfort, and IAQ (Zhang et al. 2010). The interaction between the model simulation and the optimization tool (genetic algorithm) is a continuous process until the optimum results are reached. The genetic algorithm optimizer coupled with the system simulation is shown in a flow chart presented in Figure 2. The main genetic algorithm parameters used in our simulation include a population size equal to 20 times the number of variables. The crossover fraction is set to 0.1, the elite count is set to 2; generations are set to 100; and the tolerance function is taken as 1×10^{-14}.

Solution Methodology

To perform the integrated system simulation, the physical dimensions of the space, solar-storage tank system as well as the internal loads are needed as input information. Then, the simulation will start at the first hour of operation (7 a.m.) by using the ambient conditions (dry bulb temperature, humidity ratio, and solar irradiance) and assuming initial values for the water temperature and space conditions. The optimizer will randomly seed values for the DV supply air temperature and air flow rate and regeneration air temperature. The simulation of the integrated model will then calculate the energy cost associated with the selected operational variables and will also check if the constraints are satisfied. The same process is then repeated for the entire operational hours extending from 7 a.m. till 7 p.m. in office buildings. For the rest of the daily hours between 7 p.m. and 7 a.m., the space model and the water storage tank system are simulated without the operation of the DV system to obtain the initial assumed values for the storage water temperature and space conditions. Finally, the hourly simulation is repeated over several days to obtain steady periodic solution where the difference in the initial values is less than 0.1% from one day to the other. Each month of the cooling season is represented by 1 day.

EXPERIMENTAL VALIDATION OF THE HYBRID SYSTEM MODEL

Although each of the component models of the hybrid system has followed a known and validated model in literature, it is necessary to test the validity of the integrated system model energy consumption, occupant's thermal comfort for the range of operational parameters of supply air temperature, regeneration temperature, and flow rate during the

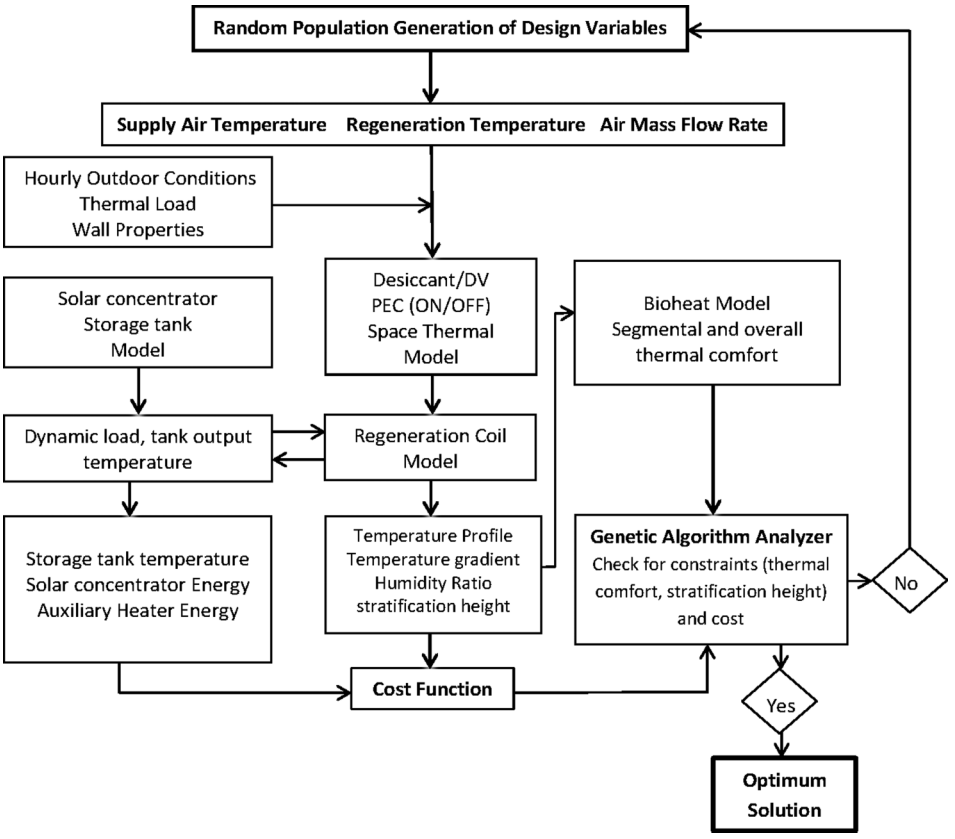

Figure 2 Optimization data flow chart.

system operation considering the inherent assumptions in each of the models. The validation of model will be done experimentally using a climatic chamber equipped with DV/SD cooling and dehumidification system. The objectives of the experiments are: (1) to compare the experimentally measured and predicted energy consumption, space thermal response, desiccant wheel exit temperature, and humidity as function of regeneration temperature and (2) to verify that thermal comfort constraint, based on participant votes, is met at all times in the space with the use of PEC during the system operation under transient space load.

Description of the Experimental Setup and Procedures

A schematic of the experimental facility is shown in Figure 3(a and b), which include a twin-room outdoor climatic chamber of dimensions 2.8 m × 2.8 m × 2.7 m, cooling coil and chiller, sensible wheel and latent SD wheel, electrically heated storage tank, supply and exhaust fans, and water pumps for the chiller and for the hot water tank. The climatic chambers' walls are highly insulated with a wall conductance of $U = 1 \pm 0.1$ W/m^2·K. The chambers have three internal walls and one external south-oriented wall. The cooling load of the space is mainly due to the internal loads. The DV air flow rate is supplied at a constant flow of 0.126 m^3/s and the control of the supply air temperature is achieved by regulating the chilled water flow rate (provided by a chiller of a 16.9 kW capacity) passing through a cooling coil using a double regulating valve. The desiccant wheel rotates at a

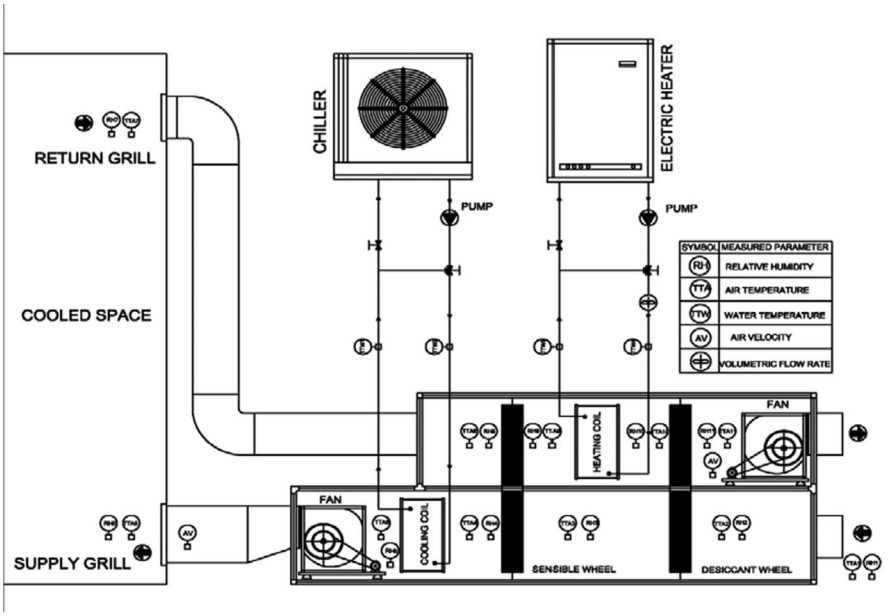

Figure 3 Schematic of (a) the experimental facility showing sensor location and (b) the twin-room climatic chamber floor plan.

speed of 6 rpm and is regenerated by raising the temperature of the chamber's return air stream using a heating coil that receives hot water from the hot water tank heated by a 6 kW electric heater with a temperature regulator of $\pm$ 1.0°C. The regeneration air temperature is controlled using a double regulating valve connected to the inlet of the heating coil.

Inside the room our main concern is the temperature and relative humidity at the supply and the return grills. The air temperature measurements are recorded inside the AHU and the supply and return ducts using QAM2161.040 duct temperature sensors with an accuracy of $\pm 0.3°C$. The relative humidity before and after the dehumidification wheel is measured using HX71-V1 sensor with an accuracy of $\pm 3.5\%$. Moreover, an OM-EL-USB-2 relative humidity and temperature logger is used to record temperature and humidity of room supply air and ambient air with an accuracy of $\pm 0.5°C$ in temperature and $\pm 3.0\%$ in relative humidity. Moreover, temperature and flow rate measurements are recorded at the inlet and the outlet of the regeneration and the cooling coils for both the air side and the water side. The water temperature is measured using an industrial rigid stem thermometer with an accuracy of $\pm 1°C$ and the water flow rate is measured using FL46300 in line flow meter with an accuracy of $\pm 5\%$. These measurements were needed to estimate thermal energy consumption in the regenerator and cooling coil in the experiments.

Experiments will be performed operating the SD and DV cooling system at three regeneration temperatures of 64°C, 72°C, and 76°C, each regeneration temperature was set for a day. The supply air temperature is fixed at 21°C and the thermal load in the space is set such that the return air temperature is $25 \pm 0.5°C$. On the day of each experiment, the system would be turned on at 8 a.m., but the actual data recording is started at 2 p.m. after ensuring that quasi-steady conditions are reached in the system. For the regeneration temperatures 72°C and 76°C, the experiments involved also human subject participation to record their thermal comfort and sensation votes on segmental and overall comfort on the nine-point scale of Zhang et al. (2010), which runs between -4 (very uncomfortable) and $+4$ (very comfortable). Four experiments are performed on two 24- year old male participants with an average weight of 75 kg and a height of 175 cm. Tests are carried with the PEC placed at distance $x = 35$ cm from the seated person and air is withdrawn at a height of 30 cm above the floor. The PEC flow rate was fixed to 10 l/s. A condition in selecting the subjects is that they should be living in Beirut. Moreover, to minimize variations due to differences in clothing, subjects were asked to wear the typical formal office clothing ensemble in Beirut. The typical clothing for males is long-sleeved shirts with long trousers having a clothing insulation of 0.6 clo. Before entering the experimental DV room, the participant is asked to sit for 1 hour in the second pre-conditioned space of the twin chambers at air temperature of 25°C to eliminate transient human body thermal effects. The participant is asked to fill the thermal comfort questionnaire after spending 1 hour inside the DV-conditioned room. The questionnaire used in this work is adapted from the questionnaire published by de Dear Cândido, Lamberts, and Bittencourt (2010) and is presented in two parts: the subjects' demographic and anthropometric characteristics, such as age, height, weight, and gender, and overall and segmental thermal sensation and discomfort. Each subject answered the questionnaire on two separate occasions during the same experiment. The experiment was repeated with two different subjects to average the reported comfort. The experiments involving participants were done simultaneously with the energy validation experiments since conditions in the conditioned space were fixed during all experiments.

Model Validation Results

The recorded weather data, space dimensions, internal load of the experiment, regenerator hot water, and DV supply air flow rates will be used as input to the integrated simulation model. In order to achieve fast steady state conditions, a simulation was run for

Table 2 Experimental and Simulation Energy Consumptions at Different Regeneration Temperatures

Regeneration temp. (°C)	Ambient temp. (°C)	Ambient humidity ratio (kg H_2O/kg air)	Cooling coil consumption (kWh)	Regenerating coil consumption (kWh)	Humidity ratio leaving dehumidifier (kg H_2O/kg air)	Temperature leaving dehumidifier (°C)	Humidity ratio supply (kg H_2O/kg air)
					Experimental		
76	33.5	0.0189	0.619 ± 0.062	1.599 ± 0.137	0.0115	53.5	0.0114
72	33.0	0.0192	0.535 ± 0.062	1.155 ± 0.122	0.0125	52	0.0121
64	32.5	0.0194	0.468 ± 0.061	1.066 ± 0.119	0.0111	48	0.0111
					Simulation		
76	33.5	0.0189	0.58	1.41	0.0104	54.5	0.0104
72	33.0	0.0192	0.50	1.32	0.0104	52.4	0.0104
64	32.5	0.0194	0.369	1.05	0.0101	49.8	0.0101

24 hours to acquire the initial conditions that will be used in the succeeding simulations. The energy consumption evaluated from measured temperatures and humidities across the cooling coil and the regenerator of the DV/SD system will be compared to values predicted by the integrated DV/SD-PEC simulation model. The experiments were conducted on July 9, 10, and 12, 2012. However, the thermal comfort experiments were performed on 2 days July 9 and 10 for two regeneration temperatures 72°C and 76°C and the supply temperature varied between 20.7°C and 21.5°C for day 1 and between 20.5°C and 21.1°C for day 2. The outdoor temperature during the operation of the experiments varied between 32.5°C and 33.5°C. The inner wall temperature measured during experiments varied between 26.8°C and 27.5°C. The recording period between 2 p.m. and 4 p.m. showed only a change of 0.5°C in ambient air temperature and return air temperature, which is within the acceptable error range for which we can consider that we have steady state operation suitable for testing the system energy performance and the participants' thermal comfort.

Table 2 presents measured and model predicted values of the regeneration energy and cooling coil thermal energy consumption in addition to the humidity ratio and air temperature at the dehumidifier exit for three values of the regeneration temperature. The highest regeneration temperature is associated with the highest energy consumption for both cooling and regeneration. Moreover, as the regeneration temperature decreases, the cooling coil energy consumption decreases due to lower temperature difference across the coil. Additionally, less energy is required to increase the water temperature passing through the regeneration coil. However, good agreement is observed between measured experimental values and integrated model predicted values of energy consumption. Table 3 presents the thermal comfort average segmental votes recorded by participants and the local thermal comfort predicted by the bioheat and thermal comfort models based on room environmental conditions and PEC flow rate. There is an excellent agreement between recorded vote and predicted segmental thermal comfort.

THE DV/SD HYBRID SYSTEM OPTIMIZATION MODEL APPLIED TO A TEST CASE IN BEIRUT CLIMATE

A case study is selected to apply the optimization procedure for the operation of the integrated DV/SD-PEC cooling systems and assess the associated energy savings when comparing system performance with the use of PEC and without the use of PEC, and with the performance of conventional system. The considered case study is an office with 8 m ×

Table 3 Experimental and Simulation Local Thermal Comfort Level on the Scale that Runs from Very Uncomfortable (−4) to Very Comfortable (+4)

Regeneration temp. (°C)	Average supply air temp. (°C)	Local thermal comfort	Head	Chest	Back	Feet
76	21.1	Subject 1	1.10	1.70	1.30	1.65
		Subject 2	0.90	1.80	1.20	1.45
		Simulation 1	0.92	1.81	1.35	1.47
72	20.8	Subject 1	1.20	1.75	1.25	1.55
		Subject 2	1.00	1.65	1.35	1.50
		Simulation 2	1.01	1.85	1.34	1.46

Table 4 Wall Layer Properties

Layer number	Layer material	Thickness (mm)	Density (kg/m^3)	Specific heat (kJ/kg-K)	Thermal conductivity	*R*-value (m^2-K/W)
1	Gypsum board	15.88	800.9	1.09	0.161	0.098
2	LW concrete block	101.59	608.7	0.84	0.38	0.266
3	Face brick	101.59	2002.3	0.92	1.33	0.076

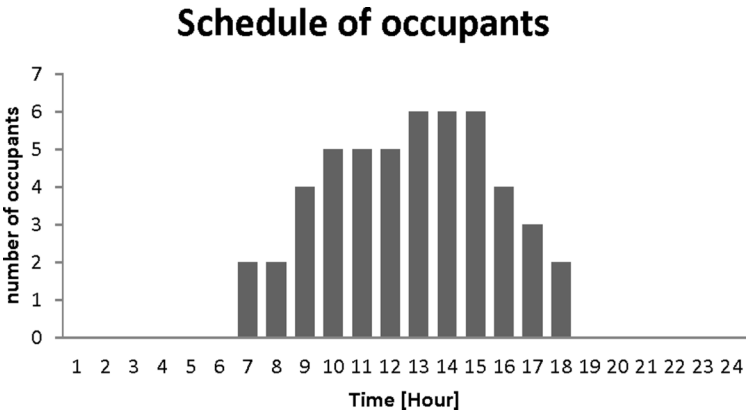

Figure 4 Occupancy schedule for a period of 24 hours.

8 m floor area and the height of the room is 3 m. The single room office is conditioned by using DV, desiccant dehumidification, and personalized evaporative cooling systems. The room consists of two external south and west walls with two partitions and the floor and ceiling are next to conditioned spaces at 25 °C. The wall configuration is a widely used wall configuration that consists of the layers listed in Table 4. The overall thickness of the wall is 219.06 mm and the overall *U*-value of the wall is 1.28 W/m^2·K. The solar flux has an impact on the external walls that are present in the building. The occupancy schedule and the internal load schedule for all the test cases are identical and are shown in Figures 4 and 5, respectively. The climate-dependent load is part of the overall thermal load and its ratio to the internal load (at peak load) is 0.5813 and at the minimum thermal load is 0.045. A solar concentrator of 6 m length connected to a 1 m^3 hot water storage tank (Audah, Ghaddar, and Ghali 2011) to supply heat to air passing for desiccant regeneration. The solar concentration system is considered since it provides high solar fraction and does not

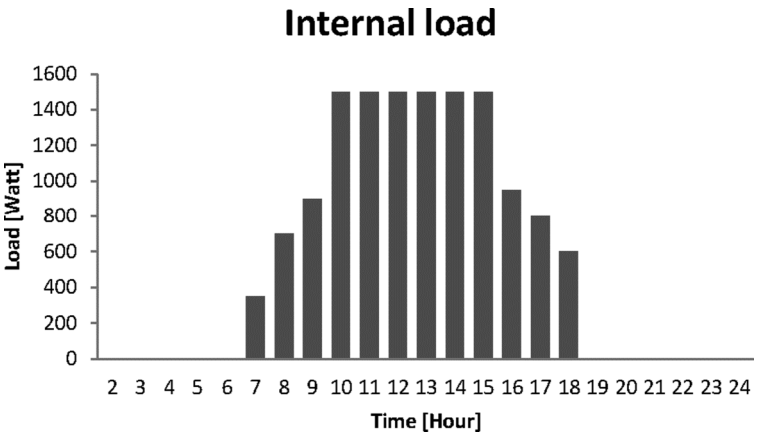

Figure 5 Internal sensible load schedule for a period of 24 hours.

Table 5 Parabolic Solar Concentrator Module Design Parameter

Parameter	Value
Length of solar concentrator	6 m
Width of solar concentrator	1.2 m
Receiver emittance	0.3
Absorber diameter	0.06 m
Transparent envelope outer diameter	0.09 m
Thickness of transparent envelope	0.004 m
Thermal conductivity of tube	16 W/m °C
Wall thickness of tube	0.05 m
Specific heat of fluid passing collector (i.e., water)	4,186 J/kg °C

occupy more than 20% of the room plan area. The specifications of the solar system are provided in Table 5.

The integrated models were simulated according to the optimized strategy A where variable supply air temperature, supply air flow rate, and regeneration air temperature at fixed PEC air flow rate. The simulations will be repeated with strategy B, the PEC flow rate is zero. The simulation will be done for all the months of the cooling season. The optimizer-simulator is run to determine the optimum values of the design variables within the range specified by the user. The upper and lower bounds for supply air range between 17°C and 25°C; for supply air flow rate range between 0.07 kg/s and 0.25 kg/s; and for regeneration temperature range between 50°C and 85°C.

RESULTS AND DISCUSSION

The DV/SD hybrid system was simulated and the developed optimization tool was used to evaluate performance and energy consumption associated with the proposed strategies for a representative day each of the cooling season months (June, July, August, September, and October).

Figure 6(a and b) shows (a) the predicted supply air temperature variations in time for strategy A with the use of PEC at flow rate of 10 l/s and (b) strategy B without the use of

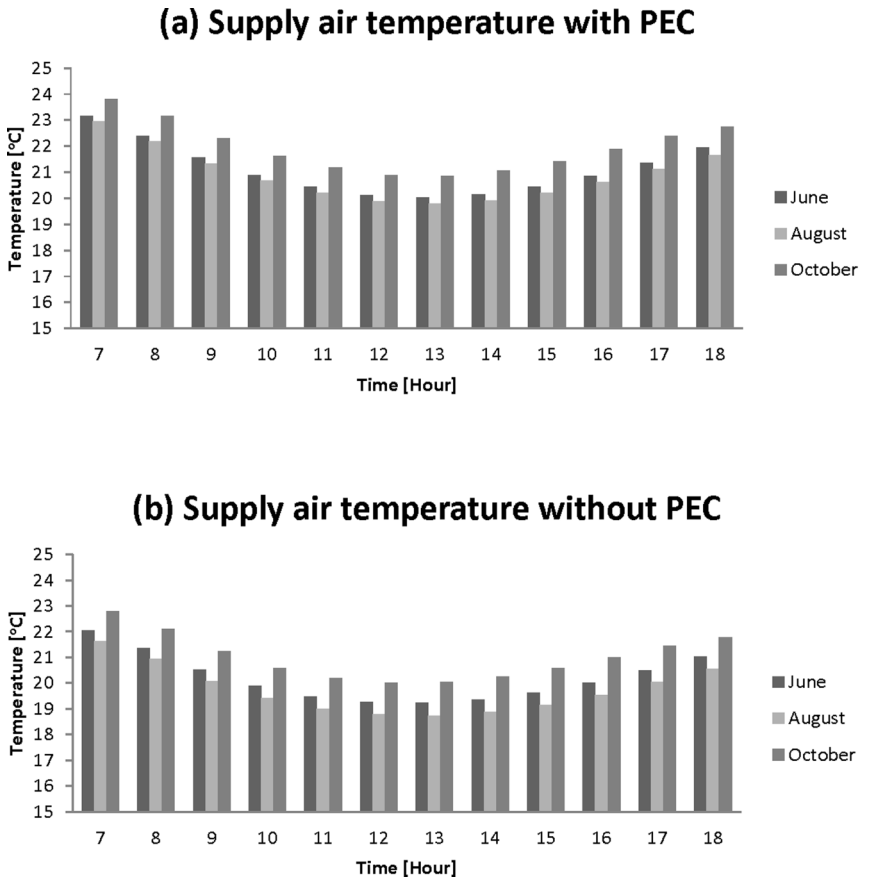

Figure 6 Supply air temperature for the hybrid system (a) with PEC and (b) without PEC.

the PEC. It is apparent that all the months follow same trend in DV supply air temperature variation throughout the day. In the early hours of the morning, the supply temperature is the highest then it drops in a decreasing slope. The lowest supply air temperature for the DV is observed in the middle of the day around 1:00 p.m. since the highest cooling load and highest occupancy are attained at this hour. The supply air temperature then keeps increasing afterward through the rest of the day. This trend in the supply air temperature variation follows the shape of variation in the internal load and the schedule of occupants. The lowest DV supply air temperature between the months is observed for the month of August where higher ambient air temperatures are attained. This increase in the external cooling load will entrain a decrease in the DV supply temperature for effective cooling and maintaining acceptable comfort conditions. The opposite phenomenon is observed for the month of October since it has the lowest ambient temperature. As seen in Figure 6(a) and 6(b), the use of the PEC modules leads to an increase in the supply air temperature between 0.8°C and 1.335°C. The use of PEC allows higher DV supply air temperatures that lead to lower chiller electrical energy consumption.

Figure 7(a and b) shows (a) the predicted regeneration temperature variations with the time of the day for (a) strategy A with the use of PEC at a flow rate of 10 l/s and (b) strategy B without the use of the PEC. Similarly, Figure 8(a and b) shows (a) the predicted

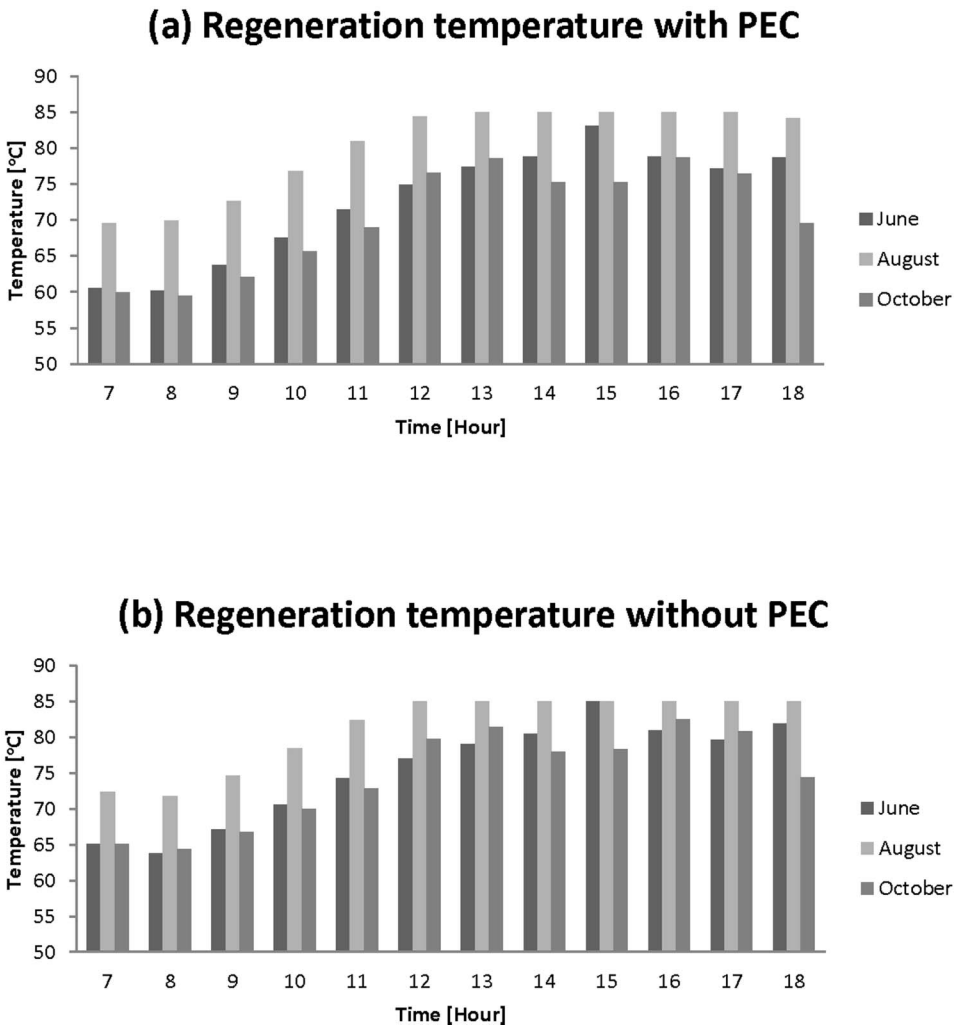

Figure 7 Regeneration temperature for the hybrid system (a) with PEC and (b) without PEC.

supply flow rate variations with time of the day for (a) strategy A and (b) strategy B. An increasing–decreasing pattern for the fresh air flow rate is observed during the working hours of the day. A low fresh air flow rate value is recorded at 7:00 a.m. in the morning and then increases with the increase of the ambient temperature and the internal load. The optimized fresh air flow rate reaches a maximum at the peak hours from 12 a.m. till 2 p.m. and then starts to decrease again. For strategy A where PEC is used, lower air flow rates were encountered compared to strategy B where the PEC modules are turned off. This reduction in the DV airflow rates leads to slightly lower regeneration air temperatures, which results in reduced energy consumption for the auxiliary unit. The month of October has lowest regeneration temperature since it has milder climatic conditions with low humidity ratios. Whereas, the month of August requires high regeneration temperature since the airflow rates and the ambient humidity ratio are the highest during summer.

A comparison of the energy consumption between DV/SD hybrid system while PEC is introduced (strategy A) and a standalone DV/SD hybrid system (strategy B) is presented

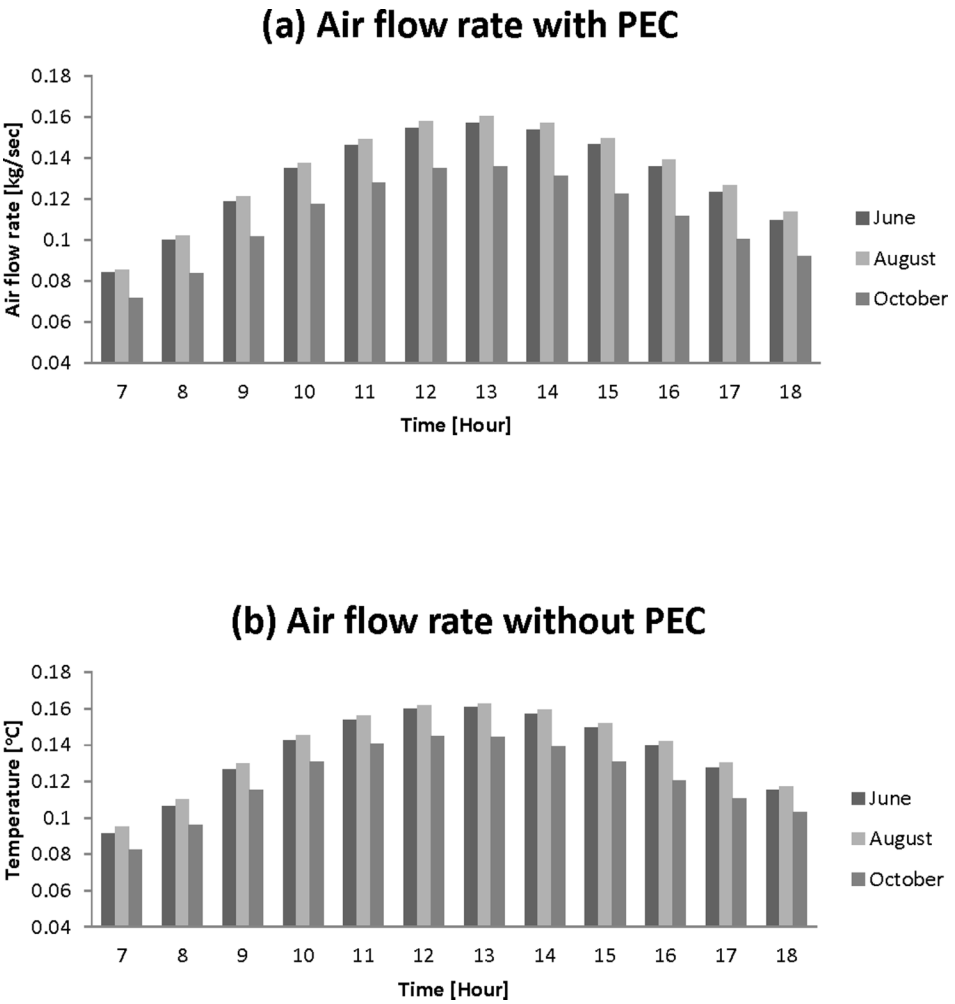

Figure 8 Air flow rate for the hybrid system (a) with PEC and (b) without PEC.

in Table 6. The chiller thermal energy is divided by the coefficient of performance with a value of 3.5 to obtain its electric energy consumption. The value of 3.5 was selected as a representative value that can encompass average value of the summer months of the given system. The coefficient of performance (COP) depends on the ambient air temperature and supply chilled water temperature. In the analysis the chilled water supply temperature is considered to be constant, thus the only variable considered is the ambient air temperature. Besides, the efficiency of the auxiliary heater is assumed to be 100% meaning that the electrical energy consumption is equal to the thermal energy consumption. Also, the fan electric power consumption is calculated based on the affinity law for prime movers. The fan power is proportional to the cube of the flow rate ratio taken with respect to a reference. The comparison showed that the use of PEC leads to an increase in the supply air temperature initiating a reduction in the chiller electrical energy consumption up to 19%. In addition, the decrease in air flow rates directly reduces the fan energy and the auxiliary energy consumption. For that reason, an energy savings up to 13.5% are obtained for the total energy consumption of the whole hybrid system. It is of interest to compare

Table 6 Energy Consumption for Strategies [A] and [B]

Month	Strategy	Electric Energy Consumption (kWh)			
		Chiller	Fan	Auxiliary	Total
June	[A]: With PEC	4.60	0.698	7.13	12.43
	[B]: Without PEC	5.49	0.782	7.83	14.10
July	[A]: With PEC	4.65	0.717	7.80	13.16
	[B]: Without PEC	5.54	0.799	8.26	14.59
August	[A]: With PEC	4.83	0.745	7.98	13.56
	[B]: Without PEC	5.72	0.824	8.55	15.10
September	[A]: With PEC	4.49	0.620	7.79	12.90
	[B]: Without PEC	5.32	0.658	8.30	14.28
October	[A]: With PEC	3.84	0.433	9.07	13.34
	[B]: Without PEC	4.49	0.561	10.09	15.14

Table 7 Thermal Comfort for Case Optimized Setting Without the PEC for Strategy [B] and Use of Same Setting of Strategy [B] While Turning the PEC On

Time (hour)	7	8	9	10	11	12	13	14	15	16	17	18
Strategy [B]	1.49	1.49	1.42	1.44	1.41	1.43	1.48	1.30	1.15	1.05	0.96	1.14
Strategy [B] + PEC	1.46	1.44	1.21	1.35	1.02	0.70	0.74	0.45	0.21	0.08	0.04	0.30

the performance of the optimized system with PEC to a reference conventional system that delivers same air quality (100% fresh air) and indoor air temperature of 24°C for the same test case and load conditions. At peak load hour, the reference conventional system electrical energy consumption is 4.6 kWh for the chiller and 1.5 kWh for the reheat resulting in a total consumption of 6.1 kWh. On the other hand, the overall energy consumption at peak hour of the optimized system with PEC is 4.156 kWh and of the optimized system without PEC is 4.58 kWh.

With the purpose of assessing the sensitivity of optimized values of the integrated hybrid system model to use of the PEC, the optimized output values of regeneration temperature, supply flow rate, and supply air temperature for strategy B are used as input to the integrated model while operating the PEC without running the genetic algorithm solver. These simulations were done with the intention of monitoring the human thermal comfort and what changes will take place if the PEC was introduced. In order to perform the assessment, the supply air temperatures and air flow rates of the DV/SD hybrid system without PEC for the month of August were considered as inputs for the space and human body models while turning the PEC on. Table 7 shows the difference in thermal discomfort for the two cases. It is clear that when the PEC is ON for an optimized strategy B, the thermal comfort deteriorates. From 7 a.m. till 11 a.m., the drop in thermal comfort is small; however after 11 a.m. it reaches values indicating uncomfortable occupants. This illustrates that combining a PEC to the hybrid desiccant/displacement system will lead to changes in the three optimized operation variables.

CONCLUSION

The optimal operational control strategy demonstrated that it is feasible to use the hybrid SD/DV system aided with PEC to provide space environmental comfort and energy

savings. A numerical modeling of the various components of the hybrid system was performed to assess its performance and to meet needed comfort conditions at 100% fresh air in Beirut humid weather. The hybrid system aided with PEC proved to save up to 13.5% of the energy consumption when operating in the optimum mode versus operating without PEC. In addition, the use of PEC has improved comfort conditions to reach desired or neutral level. Therefore, the implementation of this system in office buildings will have a large impact on the comfort of the occupants and on the quality of the air inside the space. Besides, it will allow the occupants to control their own microclimate according to their needs by varying the PEC flow rate which will contribute to reducing the percentage of people thermally dissatisfied in office spaces.

NOMENCLATURE

Symbols

AHU	air handling unit
ASHRAE	American Society of Heating Refrigeration and Air Conditioning Engineers
DV	displacement ventilation
H	stratification height, m
I	energy, kWh
IAQ	indoor air quality
PEC	personalized evaporative cooler
S	thermal sensation
SD	solid desiccant
T	Temperature, °C
RH	relative humidity
q_{PEC}	air flow rate of the personalized evaporative cooler, l/s
Q_u	useful heat gain

Greek Letters

α weighing factor

Subscripts

in	inlet
f	fan
c	cooling coil
aux	auxiliary heater
min	minimum

REFERENCES

Ahmed, M.H., N.M. Kattab, and M. Fouad. 2005. Evaluation and optimization of solar desiccant wheel performance. *Renewable Energy* 30:305–25.

ASHRAE, 2007. *ASHRAE standard 62.2-2007*. Atlanta, USA:American Society of Heating, Refrigeration, and Air Conditioning Engineers.

Audah, N., N. Ghaddar, and K. Ghali. 2011. Optimized solar-powered liquid desiccant system to supply building fresh water and cooling needs. *Applied Energy* 88:3726–36.

Ayoub, M., N. Ghaddar, and K. Ghali. 2007. Energy consumption of solar-assisted desiccant dehumidification air conditioning system in Beirut. *Kuwait Journal of Science* 34(1):107–22.

Caldas, L.G. and L.K. Norford. 2003. Genetic algorithms optimization of building envelopes and the design and control of HVAC systems. *Journal of Solar Energy Engineering* 125:343–51.

Chakroun, W., N. Ghaddar, and K. Ghali. 2011. Chilled ceiling and displacement ventilation aided with personalized evaporative cooler. *Energy and Buildings* 43:3250–7.

de Dear Cândido, R.J., R. Lamberts, and L. Bittencourt. 2010. Air movement acceptability limits and thermal comfort in Brazil's hot humid climate zone. *Building and Environment* 45(1):222–9.

Dong Chung, J., D. Lee, and S. Yoon. 2008. Optimization of desiccant wheel speed and area ratio of regeneration to dehumidification as a function of regeneration temperature. *Solar Energy* 83:625–35.

Duffie, J. and W. Beckman. 2003. *Solar engineering of thermal processes*. 3rd ed. New York:Wiley.

Fang, L., G. Clausen, and P.O. Fanger. 1998. Impact of temperature and humidity on the perception of indoor air quality. *Indoor Air* 8(2):80–90.

Ghali, K., M. Othmani, and N. Ghaddar. 2008. Energy consumption and feasibility study of a hybrid desiccant dehumidification air conditioning system in Beirut. *International Journal of Green Energy* 5(5):360–72.

Jiang, Z., Q. Chen, and A. Moser. 1992. Indoor airflow with cooling and radiative/convective heat source. *ASHRAE Transactions* 98(1):33–42.

Knoak, A., D. Coit, W. Smith, and E. Alice. 2006. Multi-objective optimization using genetic algorithms: a tutorial. *Reliability Engineering and System Safety* 91:992–1007.

Makhoul, A., K. Ghali, and N. Ghaddar. 2013. The energy saving potential and the associated thermal comfort of displacement ventilation systems assisted by personalized ventilation. *Indoor and Built Environment* 22:508–19.

Makhoul, A., K. Ghali, and N. Ghaddar. 2012. A simplified combined displacement and personalized ventilation model. *HVAC&R Research* 18:737–49.

Meckler, M. 1995. Desiccant outdoor air pre-conditioners maximize heat recovery ventilation potentials. *ASHRAE Transaction Symposia* 101:992–1000.

Melikov, A.K. 2004. Personalized ventilation. *Indoor Air* 14(Supplement 7):157–67.

Mitchell, M. 1997. *An Introduction to Genetic Algorithm*. Cambridge:The MIT Press.

Mossolly, M., N. Ghaddar, K. Ghali, and L. Jensen. 2008. Optimized operation of combined chilled ceiling displacement ventilation system using genetic algorithm. *ASHRAE Transactions* 143(2):541–54.

Salloum, M., N. Ghaddar, and K. Ghali. 2007. A new transient bioheat model of the human body and its integration to clothing models. *International Journal of Thermal Sciences* 46:371–84.

Wright, J.A., H.A. Loosemore, and R. Farmani. 2002. Optimization of building thermal design and control by multi-criterion genetic algorithm. *Energy and Buildings* 34:959–72.

Xiong, Z.Q., Y.J. Dai, and R.Z. Wang. 2010. Energy analysis of liquid desiccant dehumidification system. *International Journal of Green Energy* 7(3):241–62.

Yuan, X., Q. Chen, and L. Glicksman. 2001. A critical review of displacement ventilation. *ASHRAE Transactions* 104(1):78–90.

Zhang, H. 2003. Human thermal sensation and comfort in transient and non-uniform thermal environments. Ph.D. dissertation, University of California, Berkeley, USA.

Zhang, H., E. Arens, D. Kim, E. Buchberger, F. Bauman, and C. Huizanga. 2010. Comfort, perceived air quality, and work performance in a low-power task–ambient conditioning system. *Building and Environment* 45(1):29–39.

Zheng, G.R. and M. Zaheer-Uddin. 1996. Optimization of thermal processes in a variable air volume HVAC system. *Energy* 21(5):407–20.

Zheng, W. and W.M. Worek. 1993. Numerical simulation of combined heat and mass transfer processes in a rotary dehumidifier. *Numerical Heat Transfer: An International Journal of Computation and Methodology; Part A: Applications* 23(2):211–32.